Supplement of Atmos. Chem. Phys., 25, 2863–2894, 2025
https://doi.org/10.5194/acp-25-2863-2025-supplement

Atmospheric Chemistry and Physics
Open Access
EGU

Supplement of

Natural emissions of VOC and NO_x over Africa constrained by TROPOMI HCHO and NO_2 data using the MAGRITTEv1.1 model

Beata Opacka et al.

Correspondence to: Beata Opacka (beata.opacka@aeronomie.be) and Trissevgeni Stavrakou (jenny@aeronomie.be)

This supplement contains:

S1. Regional and temporal variability of a priori and optimised NO_x and VOC sources (Fig. S1)
S2. Top-down anthropogenic NO_x and VOC (Fig. S2)
S3. Comparison between in situ flux measurements and modelled fluxes (Table S1)
S4. Uncertainties in TROPOMI-derived UT NO_2 (Fig. S3 and S4)
S5. Optimised isoprene emissions (Fig. S5)
S6. Interannual variability of CrIS isoprene columns (2012-2020) (Fig. S6)
S7. Estimation of average isoprene emission capacities (Table S2)

S1. Regional and temporal variability of a priori and optimised NOx and VOC sources

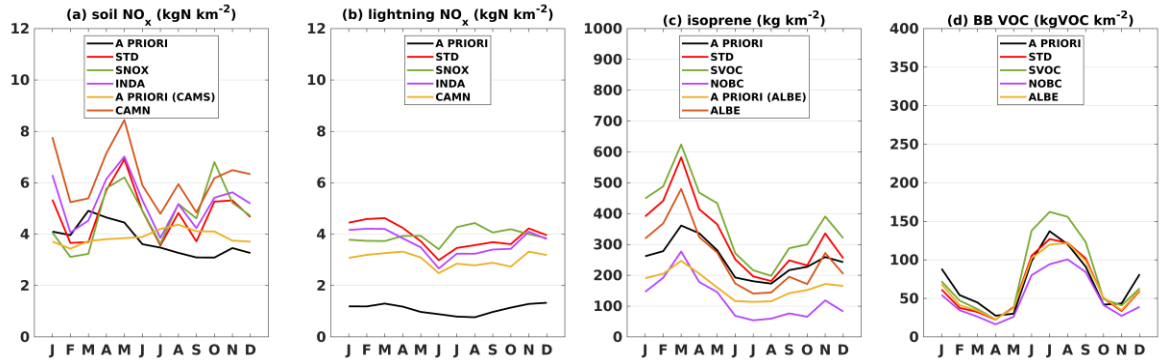

Figure S1: Seasonal variability of (a) soil NO_x (in kgN per km^2), (b) lightning NO_x (in kgN per km^2), (c) isoprene (in kg of isoprene per km^2), and (d) biomass burning VOC (in kg VOC per km^2) emissions for different inversions averaged over the entire continental domain.

S2. Top-down anthropogenic NOx and VOC

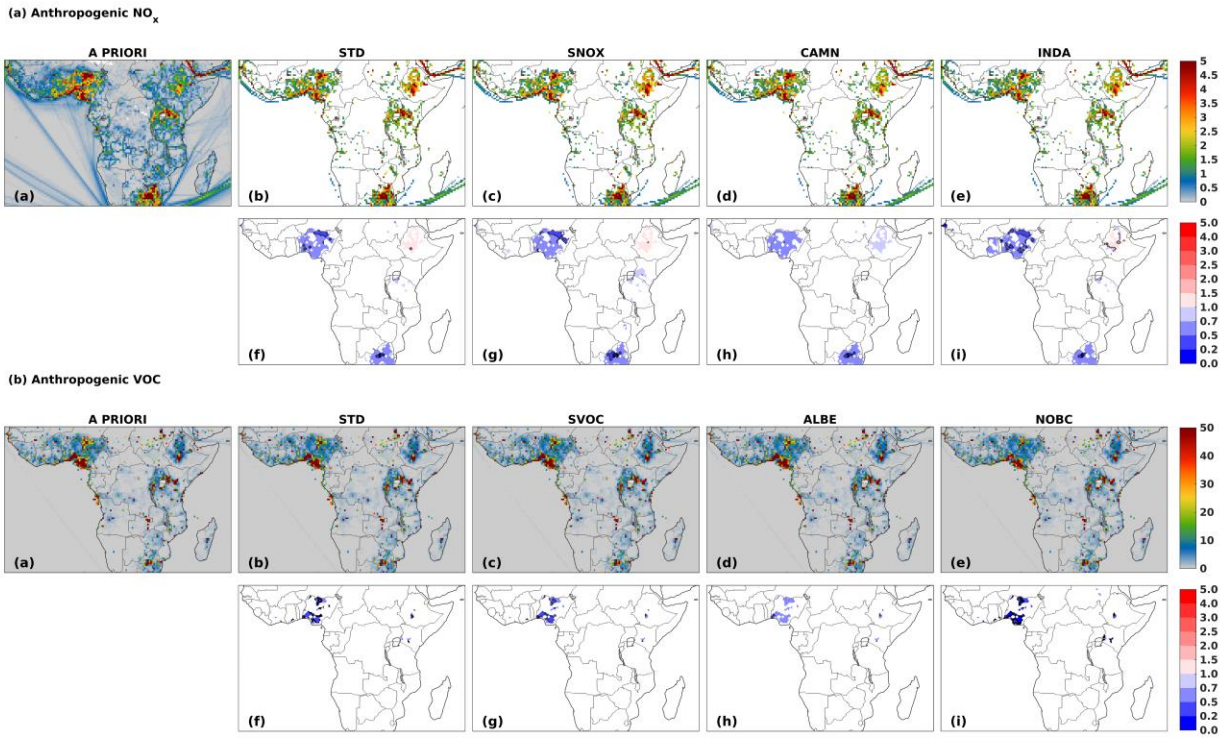

Figure S2: As in Fig. 11 and 13, but for anthropogenic (a) NO_x and (b) VOC emissions, respectively. The fluxes are expressed in in 10^{10} molec.cm^{-2} s^{-1} and the emissions increments are unitless.

S3. Comparison between in situ flux measurements and modelled fluxes

Table S1: As Table 3, with additional model estimates at each site and corresponding months. Averages over all data, as well as data in dry and wet season are provided in the table.

	Location	Month	Season	OBS	A priori	STD	INDA	CAMN (a priori)	CAMN
1	**Mayombe, Congo**	6	W	1.74	1.62	2.32	2.40	1.57	1.78
		7	D	0.78	2.28	3.73	3.48	1.52	3.03
		2	W	0.50	0.51	0.74	1.15	0.87	1.61
2	**Teke Plateau, Congo**	4	W	0.03	0.77	0.95	1.30	1.15	1.31
3	**Lamto, Ivory Coast**	1	D	1.02	2.22	1.31	6.55	2.80	1.55
		5	W	0.74	1.24	0.64	1.57	1.60	0.81
4	**Nylsvley, South Africa**	3	W	2.98	0.67	0.61	0.60	1.30	1.96
5	**KNP, South Africa**	10	W	0.97	0.85	0.46	0.46	0.20	0.19
		11	W	2.13	0.92	0.66	0.65	0.26	0.35
		12	W	1.01	0.97	1.05	1.03	0.27	0.48
		8	D	3.17	0.34	0.40	0.39	0.17	0.33
6	**Transvaal, South Africa**	9	D	1.99	0.50	0.27	0.27	0.19	0.17
7	**Marondera, Zimbabwe**	10-12	W	4.85	2.58	4.10	4.04	1.61	3.90
8	**Savè, Benin**	6-7	W	2.06	0.74	0.29	0.55	1.81	0.58
9	**Banizoumbou, Niger**	8	W	2.62	0.66	0.49	2.29	2.34	1.85
10	**Agoufou, Mali**	7	W	2.88	3.51	3.54	4.16	1.43	2.91
		8	W	0.98	0.66	0.94	1.19	2.05	4.33
11	**Dahra, Senegal**	7	W	2.45	6.05	5.58	6.12	1.42	5.13
		11	D	1.72	4.57	2.58	4.26	1.39	1.43
			Average	**1.82**	**1.67**	**1.61**	**2.23**	**1.26**	**1.77**
			Dry season average	**1.74**	**1.98**	**1.66**	**2.99**	**1.21**	**1.30**
			Wet season average	**1.85**	**1.55**	**1.60**	**1.97**	**1.28**	**1.94**

S4. Uncertainties in TROPOMI-derived UT NO_2

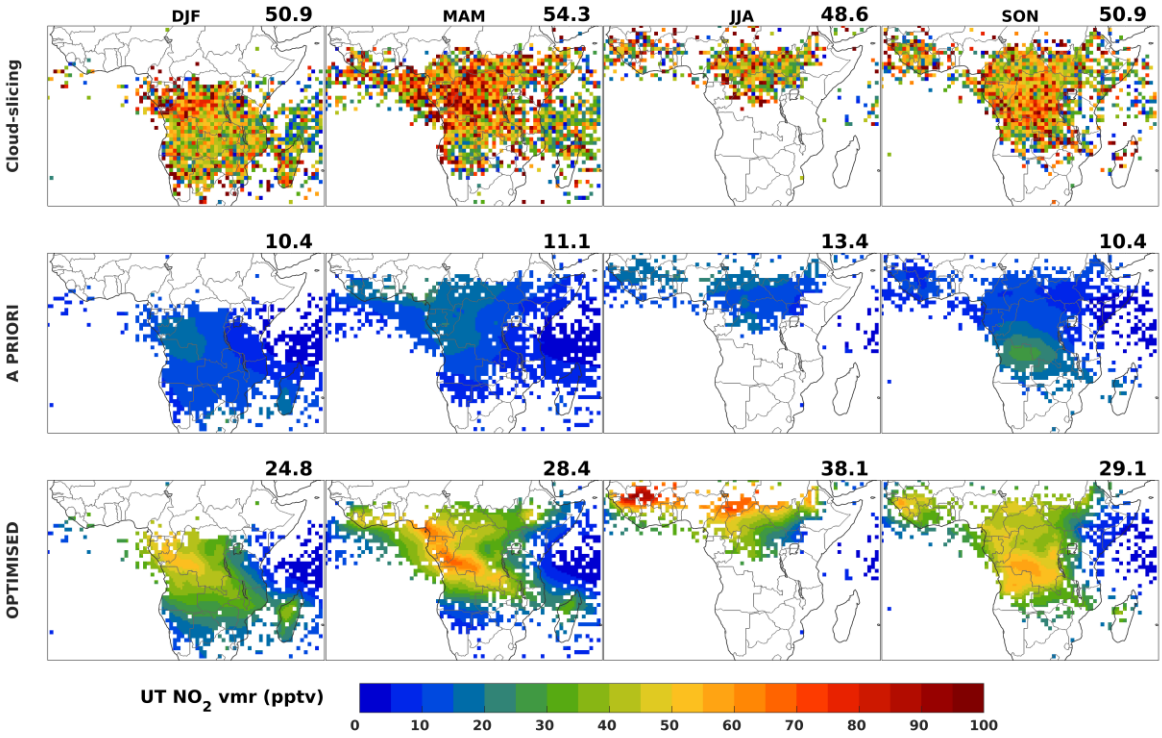

Figure S3: Seasonal distributions of upper-tropospheric NO_2 volume mixing ratios (in pptv) in December-January-February (DJF), March-April-May (MAM), June-July-August (JJA) and September-October-November (SON) from the cloud-sliced TROPOMI NO_2 over layer 320-180hPa of Horner et al. (2024) (top row), the a priori run (middle row) and the STD inversion (bottom row).

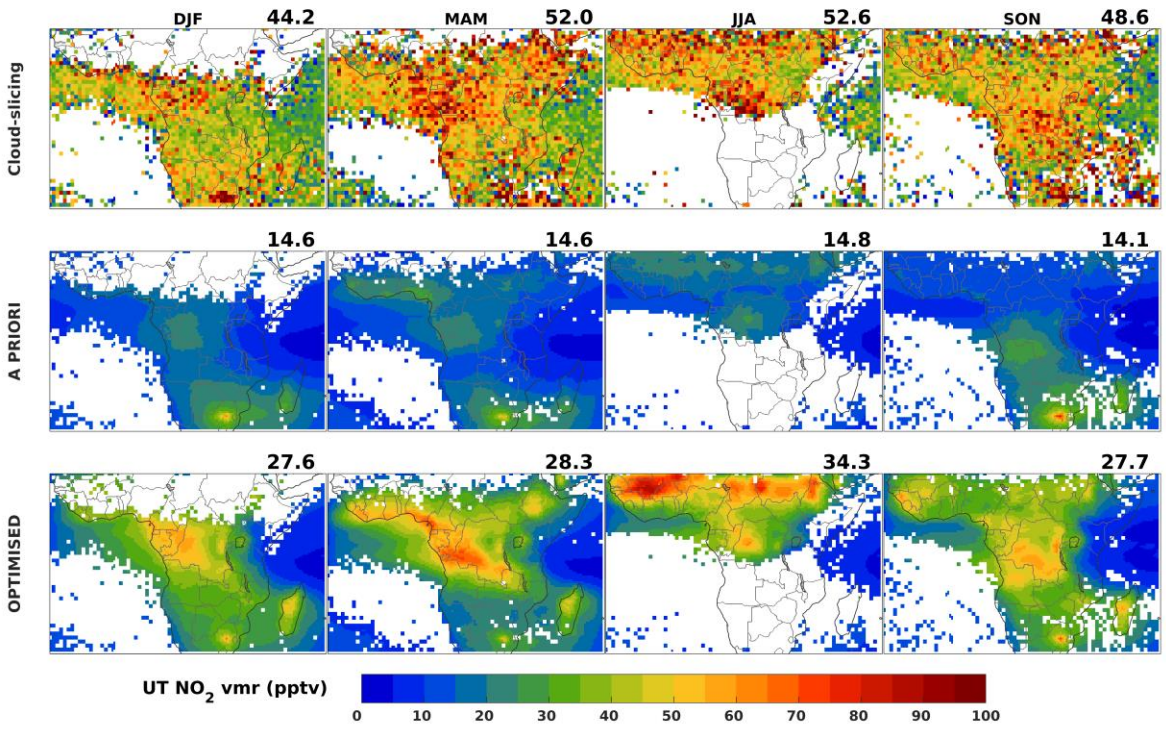

Figure S4: Same as in Fig. S3, but for layer 450-320hPa.

S5. Optimised isoprene emissions

In order to compare our STD top-down isoprene fluxes based on TROPOMI HCHO and NO_2 with the CrIS-derived isoprene fluxes from Figure S13 of Wells et al. (2020), the following figure shows the a priori and top-down STD emissions for January and April 2019.

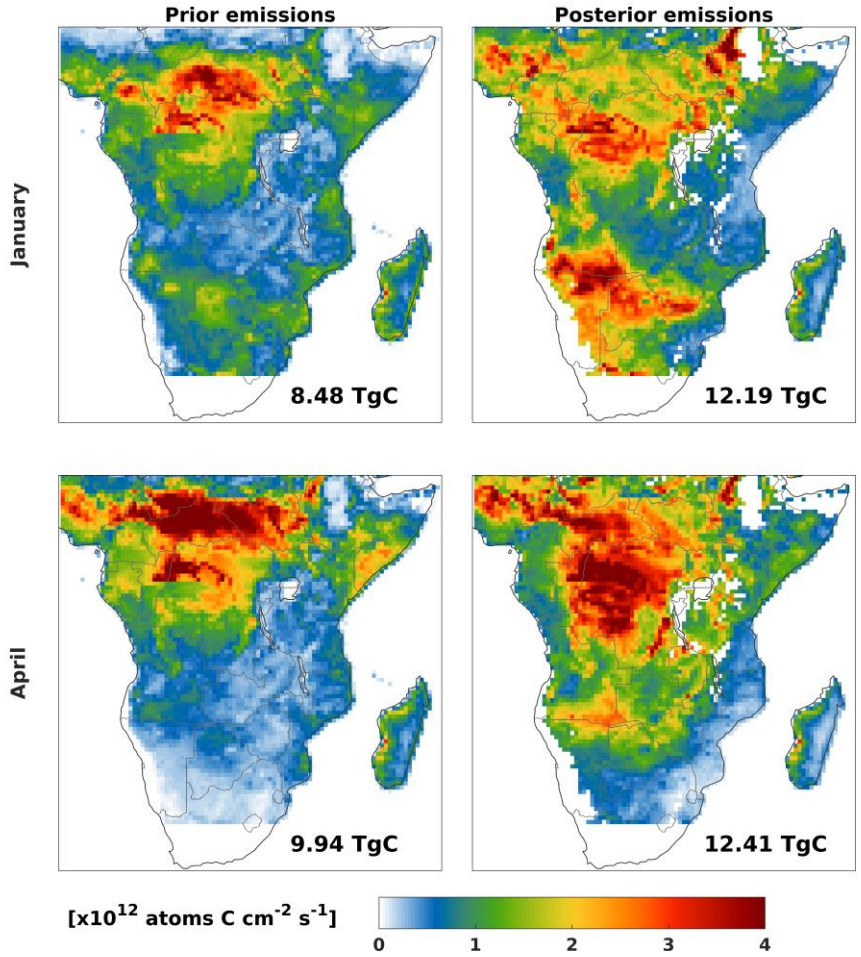

Figure S5: Spatial distribution of isoprene emissions (in 10^{12} atoms C cm^{-2} s^{-1}) from the a priori (left column) and TROPOMI-based optimisation of isoprene emissions over the same region as in Wells et al. (2020) in January (top row) and April (bottom row). Total monthly emissions are provided inset (in TgC).

S6. Interannual variability of CrIS isoprene columns (2012-2020)

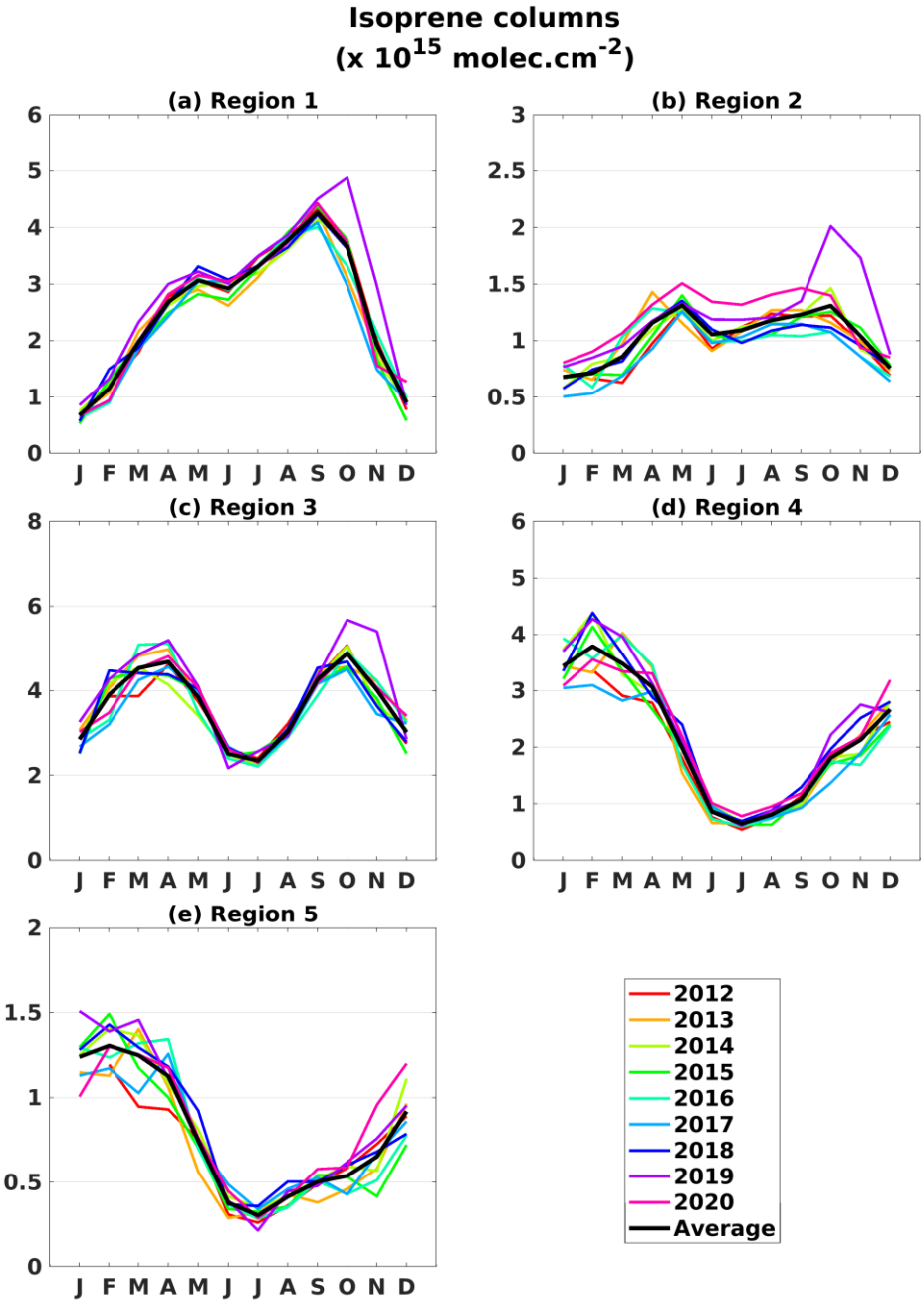

Figure S6: Time series from 2012 to 2020 of monthly isoprene columns from CrIS over the African subregions defined in Fig. 10. The average seasonal cycle for each regions over the entire 2012-2020 period is shown in black.

S7. Estimation of average isoprene emission capacities

Based on the regional isoprene emissions calculated in Tab. 4 and average isoprene emission potentials of MEGAN ($EC_{apriori}$, Guenther et al., 2012), we estimated optimised emission potential EC_{STD} from the STD inversion by proportional reasoning. Dominant ecosystems are characterised based on MODIS International Geosphere-Biosphere Programme (IGBP) classification (Sulla-Menashe et al., 2019).

Table S2: Isoprene emissions and isoprene emission capacities for the African subregions defined in Fig.10 calculated based on the a priori and optimized fluxes. Emission capacities are expressed in µg m^{-2} h^{-1}.

	Region 1	**Region 2**	**Region 3**	**Region 4**
Dominant ecosystems	*Mix of broadleaf forests and savannas*	*Shrublands and grasslands*	*Broadleaf forests*	*Mix of woody savannas and savannas*
A priori isoprene (Tg)	44	19	29	15
STD isoprene (Tg)	39	21	36	36
$EC_{apriori}$	3,700	2,900	4,100	2,500
EC_{STD}	3,300	3,200	5,100	6,000